

# Influence of Core Density and Thickness on the Behavior of Sandwich Beams under Three-Point Bending: Analytical and Experimental

Mahdi KAZEMI\*, Alireza MIRZABIGI

**Abstract:** The sandwich beams with a foam core and metal face sheets fail in mechanisms such as face sheet yield, core yield, local indentation, and face sheet folding. They can be used as impact energy absorbers in the aerospace, shipbuilding, automotive, rail industries, and elevators. This paper investigated the effect of changes in foam core density and thickness of sandwich beams using analytical methods and experimental tests through the three-point bending process. A total of 21 samples with a foam core made of polyurethane foams of different densities and thicknesses were subjected to a quasi-static three-point bending load. The load-displacement diagrams were obtained at the center of the beam using the Santam testing machine. Afterwards, the impact parameters including specific energy absorption (SEA), maximum and average forces, and efficiency coefficient were examined as the objectives of the test. The analytical and experimental bending results showed that the analytical results have good agreement with the experimental results. Also, it was found that increasing foam core thickness and density can increase the energy absorption capacity. Moreover, the results of experimental tests showed that the energy absorption capacity increased by 93.12% in the samples with the same thickness when increasing the density. Likewise, examining the samples with the same density and different thicknesses revealed that the energy absorption capacity increased by 33.37%.

**Keywords:** foam core; polyurethane foam; sandwich beam; specific energy absorption; three-point bending

## 1 INTRODUCTION

Sandwich beams are very sensitive to external loads compared to steel structures. The quasi-static loading method is suitable for determining the behavior of sandwich beams in a wide range of loading conditions. In-plane loads, three-point bending, and transverse indentation are among the loads that can be exerted in a quasi-static manner. These structures are used in cranes, bridges, frames, ship hulls, and industrial structures and have a wide application in vehicle systems. Sandwich beams are usually assembled from two or more thin and hard members as the face sheet with an intermediate thick and light core. They are capable of withstanding impact, blast, and dynamic loads. Sandwich beams have a structure with a regular core, which makes a good compromise between performance (energy absorption) and productivity. The two parameters that sandwich structures are designed based on are low weight and high strength. The core should have sufficient stiffness for the shear forces applied to the beam and can prevent the plates from slipping on each other [1, 2]. Sandwich beams with two separate face sheets and a light core are very effective under bending loads. The conventional technology of sandwich beams commonly utilizes honeycomb cores in light aerospace structures and uses foam-core polymers in building panels. The honeycomb sandwich creates lightweight high-strength structures but may cause some problems. The curved geometries are difficult to form in this type of beam and the cores are highly non-isotropic. Polymeric foams are among the cheapest materials used for the cores, which play an economically effective role in the cost-efficient production of sandwich panels. Sandwich beams with metal face sheets and foam cores can have a great influence on structures due to easier forming, isotropic core, high energy absorption, lightweight design, and high-temperature operation [3]. In recent years, the design of structures to deal with blast and impact loads has been recognized as a vital necessity [4, 5]. Lattice metal cores are the most popular core in sandwich beams for absorbing blast and indentation loads. These cores provide strength and stiffness in all directions. In addition to the high flexibility in design processes, low production costs,

and the advantage of easy manufacturing have made the sandwich structure attractive for mass production [6-7]. On the other hand, the growing interest in the use of polymeric foams as the filler to improve performance and energy absorption is one of the capabilities the sandwich beams with such cores possess [8, 9]. Therefore, extensive research has been done on the combination of cellular lattice cores with polymer foams, which increases the rate of energy absorption, acoustic, and thermal insulation [10].

The forces resulting from blast waves and the destruction caused by the collision of projectiles are a constant threat that can cause serious damage to structures and war machines [11]. In this regard, researchers have proposed structures such as sandwich panels [12] with cores composed of polymer foams [13] and metals [14] which can act as absorbers. Considerable research efforts have been made to investigate the behavior of sandwich structures in the direction of energy absorption compared to integrated structures under explosive loads [15]. The effects of different cores such as trapezoid, corrugated, honeycomb, quadrilateral, and pyramidal cores for energy absorption in sandwich beams have been investigated [16, 17]. Zhao and Hutchinson [18] showed that sandwich beams show better behavior in absorbing energy under blast loads compared to integrated beams of the same material and weight. Fleck et al. [19] analyzed sandwich plates with a three-phase model: contact phase between components, core crushing phase, and bending and stretching phase of surface plates. Tilbrook et al. [20] and Liang et al. [21] presented soft cores of low transverse strength, which greatly reduce the waves transmitted to the structure by the blast in the water and increase the coupling between the core crushing and the bending in the upper and lower plates. In these structures, the core is crushed completely and shows a high reaction. Evans et al. [22] investigated and compared the capabilities of materials in periodic cores for beams, pipes, and shells. The periodic core includes both lattice micro-truss and prismatic cores. Finally, the superior performance of the periodic cores was confirmed. The result of Evan et al.'s research was that manufacturing a regular periodic core has a higher cost. However, these types of cores improve the mechanical properties and performance of the part. Taheri-Behrooz et

al. [23] investigated the four-point bending behavior of sandwich beams with foam and resin cores at different lengths. The results of the studies showed that the failure mechanism of the beams was due to the foam indentation, followed by the failure of the shell below the load application point. Then, the load-displacement curves and the failure mechanism of the beams were compared by two experimental and numerical methods, and the results showed the high correspondence between the two methods.

Zarei and Sadighi [24] also investigated the mechanical response of a hollow honeycomb filled with polyurethane foam under the compressive loading. They used rigid polyurethane foams as the honeycomb filler phase in the tests and studied and evaluated the parameters such as the filler phase effect. Avila et al. [22] conducted studies on sandwich beams with targeted cores and proposed a criterion for the crushing of the beams. Zhang et al. (2012) [25] worked on three-point bending and pure shear in carbon fiber sandwich panels with the pyramidal core. They performed an analytical study of each loading for failure mechanisms. To construct the desired sandwich beam, they first manufactured the core and finally attached the upper composite plates to the core. In this research, they investigated different failure modes and mechanical properties of panels of different sizes (e.g., cores with different relative densities and upper plates with different thicknesses). Zhang et al. [26] studied the dynamic behavior of sandwich panels with composite shells and foam graded core under the shock load. They found that the dynamic behavior of the sandwich panel increases with the uniform increase of the foam core density from the upper plate (where it is subjected to shock load) to the back plate. Sandwich beams have various mechanisms of failure, including the core, face-sheet yield and face-sheet indentation and folding. In this paper, the initial failure forces were calculated, which occur in the event of the initial deviation of the load-displacement curve. The analysis of sandwich beams used the Deshpande and Fleck relations to predict the initial failure forces by the core yield and indentation mechanisms. The results of the analyses were compared with the results from the experimental tests of sandwich beams with aluminum face sheets and polymer foam core under three-point loading. The effect of parameters, such as foam core density and thickness, was also investigated.

## 2 ANALYSIS OF SANDWICH BEAMS

In this section, it is assumed that a sandwich beam of length  $l$  and width  $b$  is subjected to three-point bending. The characteristics of the face sheet are thickness  $t$ , Young's modulus  $E_f$ , Poisson's ratio  $\nu_f$ , and yield strength  $\sigma_{yf}$ . Also, the core characteristics are thickness  $c$ , Young's modulus  $E_c$ , shear modulus  $G_c$ , Poisson's ratio  $\nu_c$ , compressive strength  $\sigma_{yc}$ , and shear strength  $\tau_{yc}$  (Fig. 1) [3]. The bending of the beam under three-point loading is expressed by Eq. (1):

$$\delta = \frac{PL^3}{48(EI)_{eq}} + \frac{PL}{4(AG)_{eq}} \quad (1)$$

$$(EI)_{eq} = \frac{E_f bt(c+t)^2}{2} + \frac{E_f bt^3}{6} \quad (2)$$

$$(AG)_{eq} = \frac{G_c b(c+t)^2}{c} \approx G_c bc \quad (3)$$

where the amount of bending and shear stiffness are equal to:

$$\frac{E_c bc^3}{12} \approx \frac{E_f btc^2}{2}$$

The approximations have good validity considering the low thickness of the face sheet relative to the core and the proper compliance of the core with the face sheet. In a sandwich beam, several failure modes can occur: a) plastic yield of face sheets, b) folding, c) plastic yield of the core, and d) indentation of face sheet into core below the loading point. It is assumed that there is good adhesion between the face sheet and the core, which prevents delamination [3]. In the following, each of the mentioned cases will be explained.

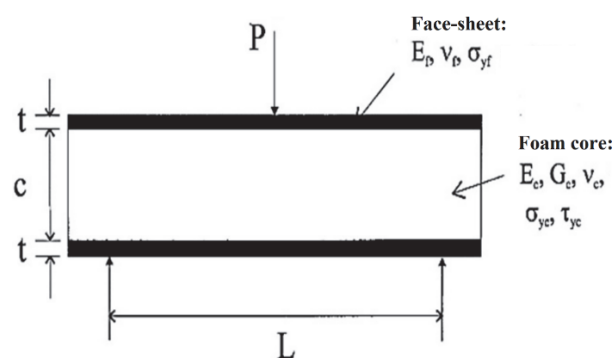


Figure 1 Schematic view of sandwich beam with face sheet and foam core parameters

### 2.1 Face-Sheet Yield

A face-sheet fails when the maximum vertical stress on the plate reaches the yield stress of the face sheet material, and the initial force can be calculated from Eq. (4).

$$P_{in\ fy} = \frac{2\sigma_{yf}btc^2}{L\left(\frac{c}{2} + t\right)} \quad (4)$$

### 2.2 Face-Sheet Folding

The folding of a face sheet occurs when the vertical stress reaches the local elastic stress or, in other words, the applied force reaches the force calculated from Eq. (5).

$$P_{fw} = 2.28E_f^{\frac{1}{3}}E_c^{\frac{2}{3}}\frac{btc}{L} \quad (5)$$

### 2.3 Core Yield

In this case, when the core reaches the yield point and when it reaches the critical point, it causes core failure and shear. Using the stress tensor in the longitudinal direction of the beam, we can write:

$$P_{in\ cy} = 2\sigma_{yc}bc \sqrt{\frac{1+(\beta/3)^2}{A^2(1-\nu'+\nu'^2)+3B^2+\beta^2A^2\left(\frac{1+\nu'}{3}\right)^2}} \quad (6)$$

where components  $A$  and  $B$  are given in Eq. (7).

$$A = \frac{E_c / E_f}{2t / L} \quad B = 1 \quad (7)$$

Also, the value of  $\nu'$  will be equal to  $\nu_c$  if it is considered at the center of the beam width with a proper approximation, and it will be equal to zero if it is examined on the core surface. Also,  $\beta$  is a constant proportional to the foam compressibility during plastic deformation, which will be equal to 2,045 [3]. In the core shear mode, given the different failure modes (Figs. 2 and 3), different mechanisms occur, each of which is separately examined below. In the first case, the hinging occurs only in the central loading (CY-A).

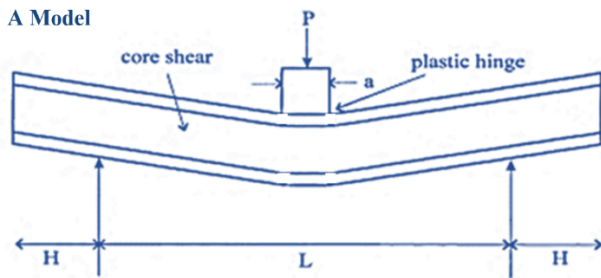


Figure 2 Hinging in center (CY-A)

However, in the second case, the hinging occurs both in the central part and in the supports (CY-B).

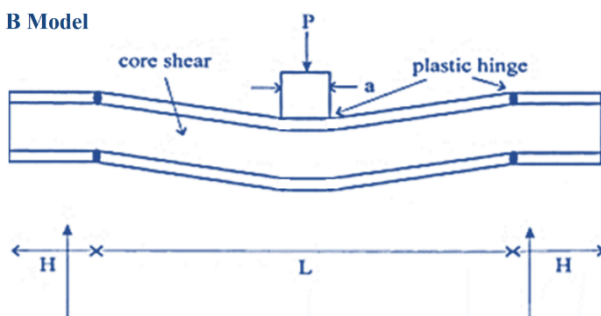


Figure 3 Hinging in center and supports (CY-B)

### 2.4 Face-Sheet Indentation

In this case, the compressive force causes the failure of the central core and also causes the main face sheet to bend.

$$P_{in} = 0.7 \left[ \sqrt{2bt} \sqrt{\sigma_{yf} \sigma_{yc}} + ab\sigma_{yc} \right] \quad (8)$$

Using the relations and  $t/L$  and  $c/L$  ratios, the prediction diagram can be obtained, which helps to find the failure mechanism of the samples. The diagram is divided into two parts, each of which presents a failure mechanism. These parts are separated by the lines that are drawn

according to the beam design mechanism. In the sandwich beams with aluminum face sheets and foam core, two parts of core indentation and shear (models A and B) are considered. The samples are displayed on the curve. This diagram is shown in Fig. 4. According to the research nature, which is the three-point bending, the face sheet and the core between the face sheets experience different failure modes and mechanisms, which were briefly mentioned above. In this study, all the forces that cause each of the failure mechanisms were calculated and then analyzed to predict the failure modes.

Due to the existence of different foam densities, Eq. (9) is used to calculate the density of sandwich beams:

$$\rho_{co} = \nu_A \rho_A + \rho_c (1 - \nu_A) \quad (9)$$

where the average relative density of the sandwich beam  $\rho_a / \rho = \rho_{co}$  is expressed as Eq. (10):

$$\bar{\rho} = \frac{2t_f + h_c \rho_c / \rho_A}{2t_f + h_c} \quad (10)$$

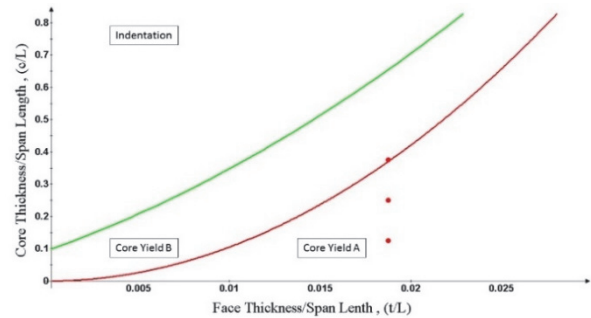


Figure 4 Prediction of failure mechanism

In this case, the forces  $\tilde{F}$  and their stiffness  $\tilde{E}$  were investigated with respect to density [27].

$$\tilde{E} = \frac{F / \delta}{\bar{\rho}} \quad (11)$$

$$\tilde{F} = \frac{F}{\sigma_y b l \bar{\rho}}$$

The comparative results are presented in the following sections.

## 3 EXPERIMENTAL TESTS

### 3.1 Material Properties

**Sandwich beams:** Sandwich beams are actually made up of two main parts: 1) low-density intermediate core, which is light and usually large, and 2) face sheets on either side of the core, which are hard and usually thin. The intermediate core is generally made of foam, cork, and honeycomb, and the face sheets on either side of the core are typically made of metals such as aluminum, composite, or their combination, namely composite metal structure. In this research, aluminum face sheets and polyurethane foam core were used to construct sandwich panels.

**Face sheets:** To prepare all samples, the cold-rolled aluminum sheet 1050 was used. To investigate the

mechanical properties of the sheets using the ASTM E08M-04 standard, three standard samples were subjected to tensile tests, and the results of the average mechanical properties are given in Fig. 5 and Tab. 1.

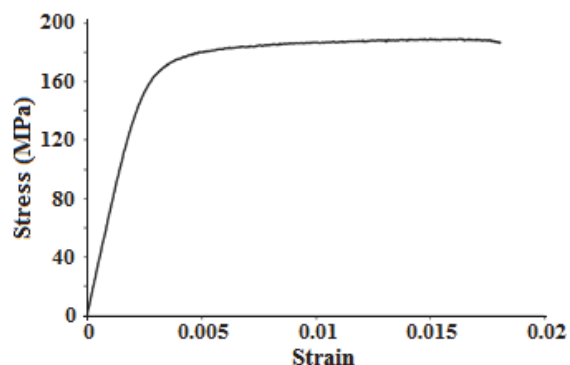


Figure 5 Tensile stress-strain curve of Al-1050 aluminum sheet

Table 1 Properties of face sheet material

| Mat.    | Thick, $h_f$ / mm | Density, $\rho$ / kg/m <sup>3</sup> | Young's modulus, $E$ / GPa | Poissons ratio, $\nu$ | Yield strength, $\sigma_y$ / MPa | Fracture strain, $\epsilon_f$ |
|---------|-------------------|-------------------------------------|----------------------------|-----------------------|----------------------------------|-------------------------------|
| Al-1050 | 1,5               | 2700                                | 70,01                      | 0,3                   | 155,5                            | 0,018                         |

**Polyurethane foam:** The core of sandwich beams was made of closed cells polyurethane foam. ASTM D1621-00 standard was used to determine the mechanical behavior of polyurethane foam [17]. Fig. 6 shows the images of polyurethane foams.

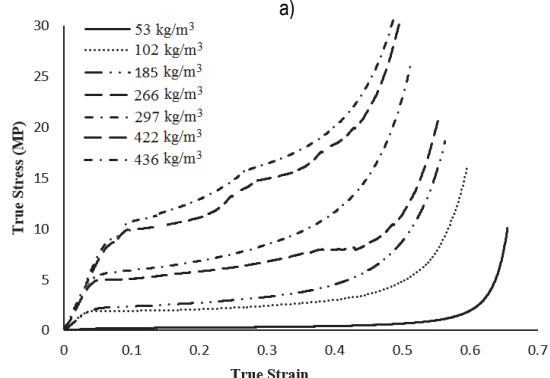
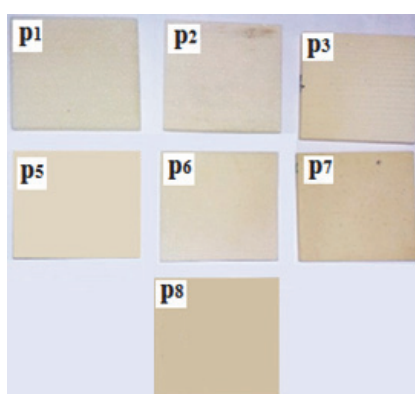


Figure 6 a) Polyurethane foams with different densities; b) Compressive curves of polyurethane foams

### 3.2 Sample Preparation

The tested sandwich structures consisted of two aluminum plates as the face sheet and a polyurethane foam

core. The face sheets were manufactured with a thickness of 1,5 mm and the foam cores with thicknesses of 10, 20, and 30 mm and densities of  $\rho_1, \rho_2, \rho_3, \rho_5, \rho_6, \rho_7,$  and  $\rho_8$  corresponding to 53,26; 102,03; 185,22; 266,17; 297,41; 422,16 and 436,7 kg/m<sup>3</sup>. The epoxy adhesive was used to connect the face sheets to the core and the core layers to each other. Fig. 7 presents the samples prepared, and Tab. 3 presents the physical characteristics of the samples.

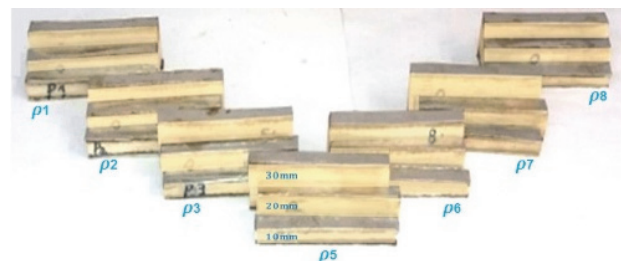


Figure 7 Prepared sandwich panel samples

### 3.3 Coding of Samples

The coding of samples generally consists of a maximum of one letter and two numbers, where the letter B represents a beam with a polyurethane core. The first number indicates the type of foam core density and the second number indicates the thickness of the foam core (cm). Tab. 2 lists the codes selected for the samples.

Table 2 Specifications and codes related to sandwich beams

| Samples | Density of core | Thickness of core / cm |
|---------|-----------------|------------------------|
| B1-1    | $\rho_1$        | 1                      |
| B1-2    | $\rho_1$        | 2                      |
| B1-3    | $\rho_1$        | 3                      |
| B2-1    | $\rho_2$        | 1                      |
| B2-2    | $\rho_2$        | 2                      |
| B2-3    | $\rho_2$        | 3                      |
| B3-1    | $\rho_3$        | 1                      |
| B3-2    | $\rho_3$        | 2                      |
| B3-3    | $\rho_3$        | 3                      |
| B5-1    | $\rho_5$        | 1                      |
| B5-2    | $\rho_5$        | 2                      |
| B5-3    | $\rho_5$        | 3                      |
| B6-1    | $\rho_6$        | 1                      |
| B6-2    | $\rho_6$        | 2                      |
| B6-3    | $\rho_6$        | 3                      |
| B7-1    | $\rho_7$        | 1                      |
| B7-2    | $\rho_7$        | 2                      |
| B7-3    | $\rho_7$        | 3                      |
| B8-1    | $\rho_8$        | 1                      |
| B8-2    | $\rho_8$        | 2                      |
| B8-3    | $\rho_8$        | 3                      |

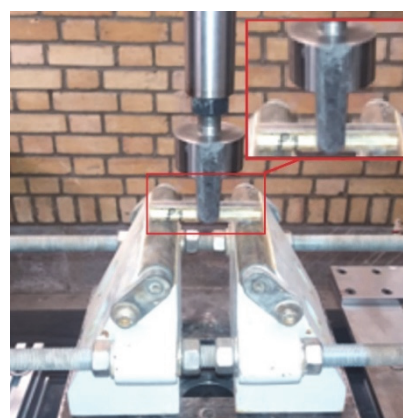


Figure 8 View of pressure device and placement of considered sample

All quasi-static bending tests were performed on foam-core sandwich beams using the universal testing machine Santam STM-250, as shown in Fig. 8. It should be noted that all samples are subjected to the quasi-static bending force at a rate of 5 mm/min.

**4 RESULTS AND DISCUSSION**

**4.1 Experimental Results**

In the study of the crushing of sandwich beams with different foam cores according to Fig. 8, given the identical thickness of the samples, it is observed that the density is very effective in load bearing. For example, sample B1-1 is not able to withstand much force due to the lower strength and lower resistance to vertical stresses and local buckling compared to sample B8-1 and other models. Conversely, in sample B8-1, the ability to absorb force greatly increases.

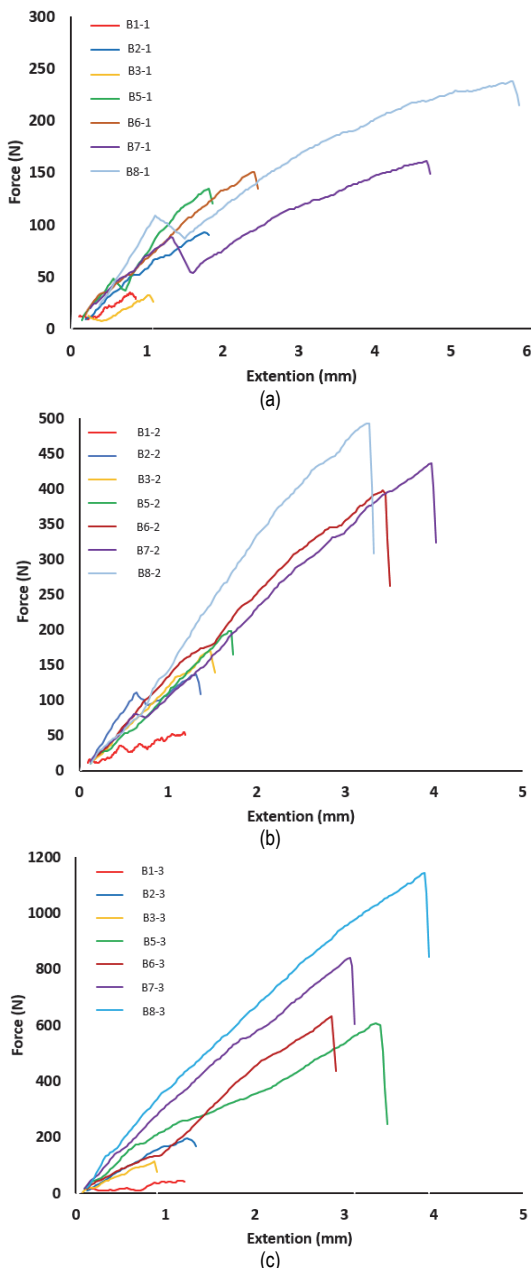


**Figure 9** Load-displacement diagrams for samples with different densities and same thickness: a) 10 mm; b) 20 mm; c) 30 mm

Also, Fig. 9 shows that the resistance of the core to the applied loads increases with increasing the density of the foam core. However, the notable point in Fig. 9 is that with increasing the thickness of the foam cores in the sandwich beams while significantly increasing the resistance to the applied load, the diagram moves towards uniformity and linearity.

Fig. 10 also shows the comparison between sandwich beams of different thicknesses under three-point bending. As can be seen in Fig. 10, the previous results are well evident. The results from the diagrams of Fig. 10, which are the same for different thicknesses at the same density, also confirm the accuracy of the obtained results.

**4.2 Energy Absorption Parameters**

Energy absorption, ( $E$ ), initial peak load ( $P_{peak}$ ), average load ( $P_{ave}$ ), and crushing force efficiency (CFE) are the main parameters that measure the properties of absorbers. In addition, there is another parameter that is of great importance in the investigation of absorbers, which is called the energy absorbed per unit weight (specific energy absorption,  $SEA$ ). Eqs. (12) to (15) are the relations of energy absorption, average force, specific energy absorption, and crushing force efficiency, respectively. These parameters are very important in the design absorber, and mass is a limiting factor. Energy absorption is the area under the load-displacement diagram. Crushing force efficiency is obtained from the ratio of the mean load to the initial peak load.

$$E_{int} = \int P d\delta_{eff} \tag{12}$$

$$P_m = \frac{E}{\delta} = \frac{\int P d\delta}{\delta} \tag{13}$$

$$CFE = \frac{P_m}{P_{max}} \tag{14}$$

$$SEA = \frac{E_{int}}{M} = \frac{\int P d\delta_{eff}}{M} \tag{15}$$

**Table 3** Energy absorption parameters

| Samples | $P_{peak} / N$ | $E / J$ | $SEA / J/kg$ | $P_{ave} / N$ | $CFE$ |
|---------|----------------|---------|--------------|---------------|-------|
| B1-1    | 42,9           | 17,36   | 2011,26      | 20,16         | 0,47  |
| B1-2    | 61,3           | 38,53   | 4204,97      | 32,28         | 0,52  |
| B1-3    | 52,3           | 27,81   | 2868,68      | 22,86         | 0,43  |
| B2-1    | 98,1           | 100     | 10996,05     | 55,28         | 0,56  |
| B2-2    | 147,2          | 120,42  | 11875,82     | 87,73         | 0,59  |
| B2-3    | 202,3          | 150,53  | 13487,77     | 111,78        | 0,55  |
| B3-1    | 42,9           | 19,28   | 1970,93      | 17,73         | 0,41  |
| B3-2    | 171,7          | 139,49  | 12167,50     | 91,23         | 0,53  |
| B3-3    | 116,5          | 53,23   | 4049,68      | 58,84         | 0,50  |
| B5-1    | 141            | 137,46  | 12773,4      | 73,64         | 0,52  |
| B5-2    | 202,3          | 174,60  | 13007,28     | 100,54        | 0,49  |
| B5-3    | 613,1          | 1118,3  | 69526,80     | 321,40        | 0,52  |
| B6-1    | 153,3          | 213,89  | 19315,22     | 86,78         | 0,56  |
| B6-2    | 404,7          | 761,20  | 54185,18     | 217,20        | 0,53  |
| B6-3    | 643,8          | 886,88  | 52101,36     | 305,09        | 0,47  |
| B7-1    | 165,5          | 466,30  | 37847,92     | 98,63         | 0,59  |
| B7-2    | 441,5          | 925     | 55928,84     | 229,85        | 0,52  |
| B7-3    | 846,1          | 1410,79 | 67951,41     | 452,96        | 0,53  |
| B8-1    | 251,4          | 925,91  | 74268,88     | 157,01        | 0,62  |
| B8-2    | 496,6          | 868,93  | 51617,98     | 261,45        | 0,52  |
| B8-3    | 1146,5         | 2533,67 | 119507,23    | 642,02        | 0,55  |



The results calculated from the experimental test of the samples are given in Tab. 3. Also, the bar charts for comparing different parameters are also given in Figs. 11 to 13. The description of the related results is given as follows.

In an overall comparison, the results of three-point bending tests showed that the energy absorption capacity of a metal sandwich beam with a foam core in the samples of the same thickness (10 mm) increased by 93,12% with increasing the density, which is equal to 88,45% in the beams with a thickness of 20 mm. In a case that was

performed at the same density ( $\rho_1$ ) and different thicknesses, the energy absorption capacity increased by 33,37%. Regarding the SEA, in the samples with the same thickness (30 mm), this value increases by 97,59% with increasing the density, which is equal to 37,85% at a constant density ( $\rho_8$ ) and different thicknesses. In the case of the maximum load for a case with the same thickness (10 mm), this value increases by 85,39% with increasing the density, and at a constant density ( $\rho_6$ ) with different thicknesses, this value is equal to 76,18%.

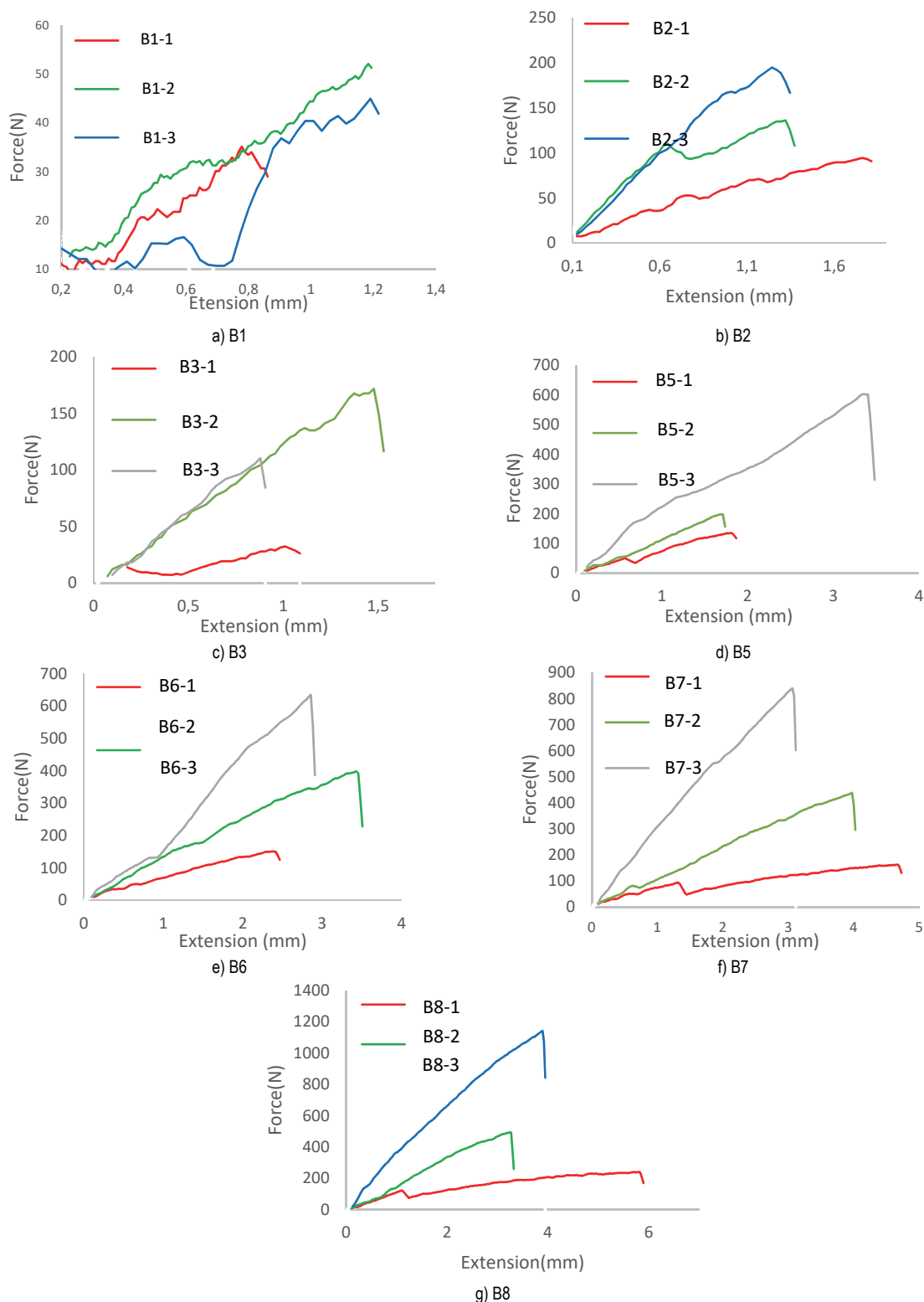


Figure 10 Load-displacement diagram for samples with same density and different thicknesses

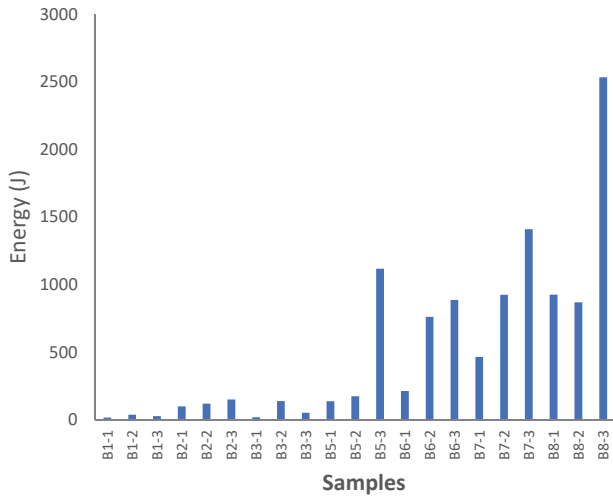


Figure 11 Energy (E) comparison diagram for different samples

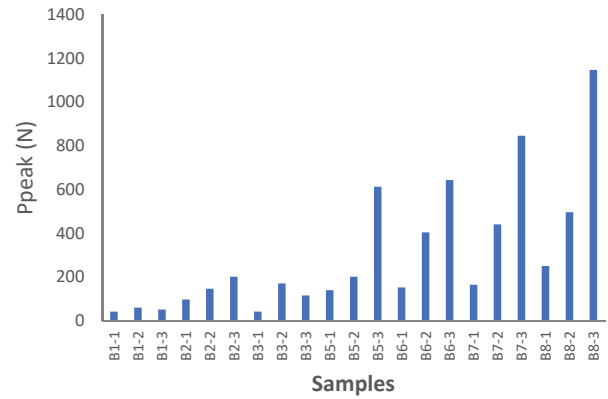


Figure 13  $P_{peak}$  comparison diagram for different samples

### 4.3 Comparison between Analytical and Experimental Results

In this section, the values of panel strength and forces according to the foam core density and thickness are given in Tab. 4. The amount of force and stiffness of each sample with respect to the relative density relation examined in the theory section and also the experimental results of the sandwich beams are obtained and given in Tab. 4. Also, the initial failure modes and mechanisms were predicted by previous relations and reported according to the sample code. Finally, it can be concluded that there is a good agreement between the results of theoretical relations and the results of experimental tests. Fig. 14 shows the failure of the foam-core sandwich panels in a sample. It can be seen that in the foam cores with lower densities while having lower load bearing, they go through a longer process until the core yield. The results are shown in Fig. 14, which is selected from the images that are taken from the samples at thirty-second intervals. However, with increasing the density and thickness of the sandwich panel while increasing the load-bearing resistance, the crack growth occurs much more intensely during the core yield, and the core suddenly fails.

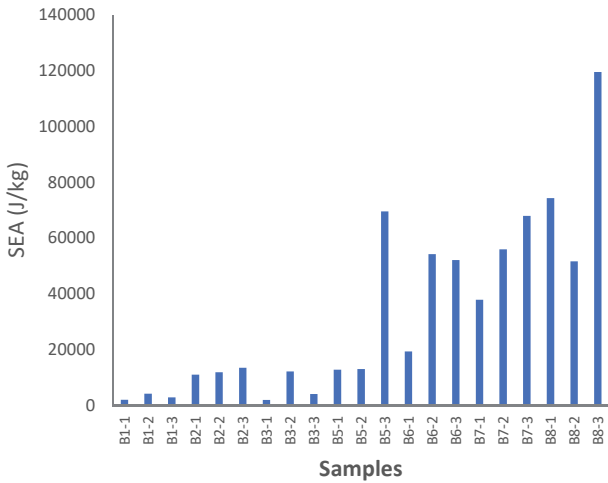


Figure 12 SEA comparison diagram for different samples

Table 4 Comparison between theoretical and experimental strength and stiffness

| N    | Failure mode | $\tilde{E} / \text{N/mm}^2$ | $\tilde{E} / \text{N/mm}^2$ | Difference / % | $\tilde{F} / \times 10^2$ | $\tilde{F} / \times 10^2$ | Difference / % |
|------|--------------|-----------------------------|-----------------------------|----------------|---------------------------|---------------------------|----------------|
|      |              | Anal.                       | Exp.                        |                | Anal.                     | Exp.                      |                |
| B1-1 | CY-A         | 3,74                        | 3,47                        | 7,3            | 0,53                      | 0,39                      | 25,8           |
| B2-1 | CY-A         | 3,62                        | 3,35                        | 7,4            | 0,52                      | 0,47                      | 9,2            |
| B3-1 | CY-A         | 3,46                        | 3,23                        | 6,5            | 0,49                      | 0,4                       | 17,1           |
| B5-1 | CY-A         | 3,25                        | 3,05                        | 5,9            | 0,46                      | 0,39                      | 16,7           |
| B6-1 | CY-A         | 3,18                        | 3,01                        | 5,8            | 0,46                      | 0,40                      | 12,1           |
| B7-1 | CY-A         | 2,96                        | 2,80                        | 5,4            | 0,45                      | 0,40                      | 11,08          |
| B8-1 | CY-A         | 2,93                        | 2,78                        | 5,4            | 0,42                      | 0,36                      | 14,2           |
| B1-2 | CY-A         | 3,74                        | 3,49                        | 6,7            | 0,94                      | 0,78                      | 17,1           |
| B2-2 | CY-A         | 3,62                        | 3,38                        | 6,5            | 0,95                      | 0,91                      | 4              |
| B3-2 | CY-A         | 3,46                        | 3,24                        | 6,3            | 0,88                      | 0,76                      | 12,7           |
| B5-2 | CY-A         | 3,25                        | 3,07                        | 5,3            | 0,83                      | 0,74                      | 10,01          |
| B6-2 | CY-A         | 3,18                        | 3,01                        | 5,5            | 1,44                      | 1,16                      | 19,5           |
| B7-2 | CY-A         | 2,96                        | 2,83                        | 4,4            | 0,76                      | 0,68                      | 10,1           |
| B8-2 | CY-A         | 2,93                        | 2,84                        | 3,3            | 0,89                      | 0,78                      | 12,7           |
| B1-3 | CY-B         | 3,74                        | 3,46                        | 7,5            | 1,82                      | 1,12                      | 11,7           |
| B2-3 | CY-B         | 3,62                        | 3,42                        | 5,4            | 1,55                      | 1,23                      | 20,9           |
| B3-3 | CY-B         | 3,46                        | 3,25                        | 6,01           | 1,49                      | 1,35                      | 9,2            |
| B5-3 | CY-B         | 3,25                        | 3,14                        | 3,1            | 2,08                      | 1,80                      | 13,04          |
| B6-3 | CY-B         | 3,18                        | 3,01                        | 5,3            | 1,38                      | 1,15                      | 16,7           |
| B7-3 | CY-B         | 2,96                        | 2,89                        | 2,4            | 1,29                      | 1,09                      | 14,8           |
| B8-3 | CY-B         | 2,93                        | 2,78                        | 5,4            | 2,54                      | 1,88                      | 26,1           |

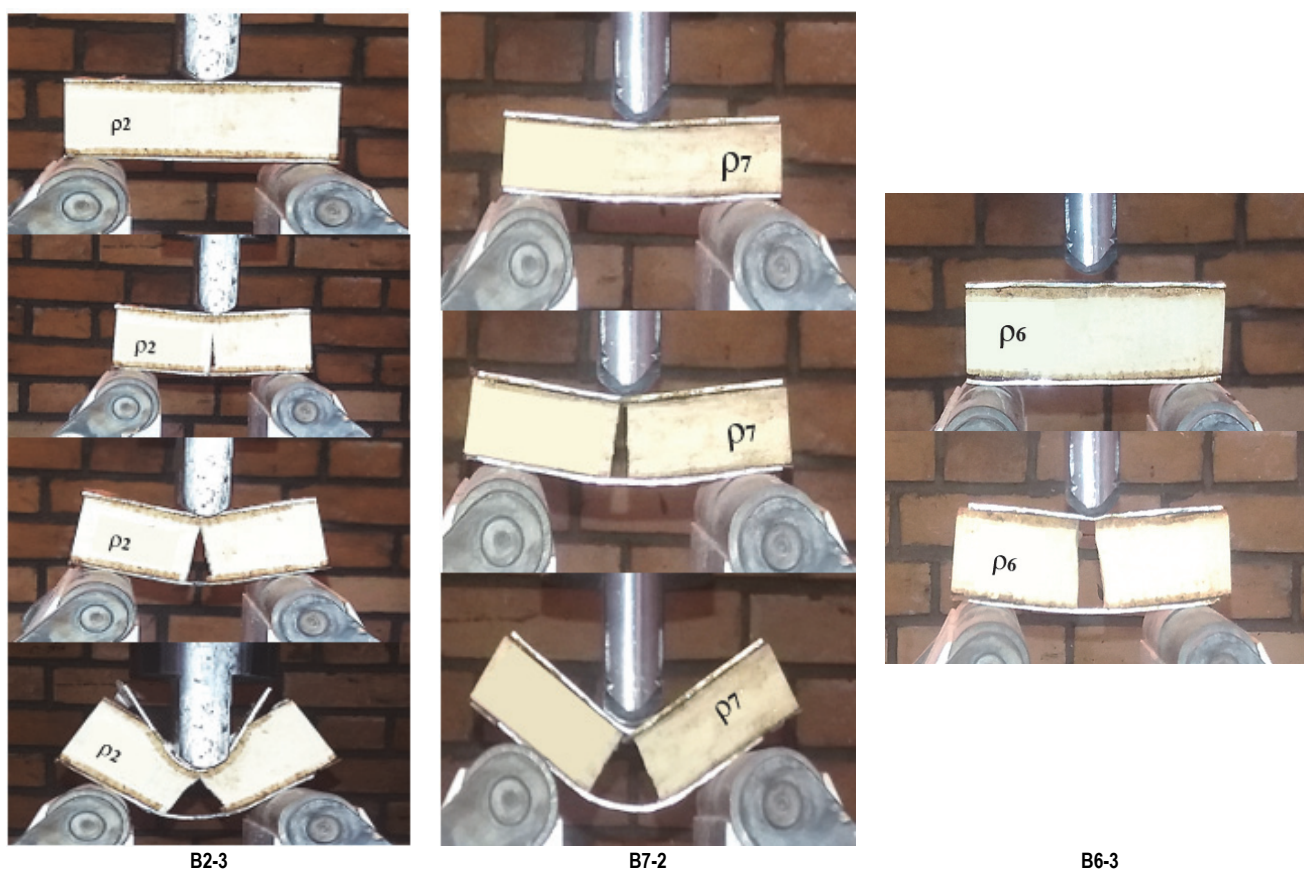


Figure 14 Failure mechanism of sandwich beams

## 5 CONCLUSION

As mentioned, sandwich beams fail due to various mechanisms. This paper attempts to examine the behavior of sandwich beams with metal face sheets and foam cores using analytical and experimental methods, taking different thicknesses and densities into account. The sandwich beams are analyzed using the Deshpande and Fleck relations, and the initial force and amount of stiffness are obtained from the given relations. The results are compared with those obtained from the experimental tests, which show an acceptable agreement. The results of the experimental tests are analyzed in the form of diagrams in different categories (in terms of constant density and constant thickness). Additionally, the parameters of energy absorption and specific energy absorption are obtained and studied according to load-displacement diagrams. It is observed that with an increase in density and thickness, the initial force increases, and the sandwich beam can withstand higher loads. It is also observed that with an increase in density and thickness, crack growth sharply increases after reaching the yield point. Finally, it can be concluded that in samples with the same thickness (10 mm), the energy absorption increases by 93.12% with an increase in density, and it is equal to 88.45% in the beams with a thickness of 20 mm. In a case where the same density ( $\rho_1$ ) is performed at different thicknesses, the energy absorption capacity increases by 33.37%. In general, it can be stated that the effect of increased density on the energy absorption parameters is much greater than the effect of increased thickness of foam cores.

## 6 REFERENCES

- [1] Guruprasad, S. & Mukherjee, A. (2000). Layered sacrificial claddings under blast loading Part I-analytical studies. *International Journal of Impact Engineering*, 24(9), 975-984. [https://doi.org/10.1016/S0734-743X\(00\)00004-X](https://doi.org/10.1016/S0734-743X(00)00004-X)
- [2] Alavi Nia, A. & Kazemi, M. (2019). Analytical and numerical investigations on the penetration of rigid projectiles into the foam core sandwich panels with aluminum face-sheets. *Proceedings of the Institution of Mechanical Engineers, Part G: Journal of Aerospace Engineering*, 233(1), 285-298. <https://doi.org/10.1177/0954410017730090>
- [3] Belan, J., Kuchariková, L., Tillová, E., & Vaško, A. (2017). The influence of applied heat-treatment on in 718 fatigue life at three point flexural bending. *Metalurgija*, 56(2), 167-170.
- [4] Wadley Hng, E. A. & Fleck, N. A. (2003). Fabrication and structural performance of periodic cellular metal sandwich structures. *Composites Science and Technology*, 63(1), 2331-2343. [https://doi.org/10.1016/S0266-3538\(03\)00266-5](https://doi.org/10.1016/S0266-3538(03)00266-5)
- [5] Deshpande, F. N. (2001). Collapse of truss core sandwich beams in 3-point bending. *International Journal of Solids and Structures*, 38(1), 6275-6305. [https://doi.org/10.1016/S0020-7683\(01\)00103-2](https://doi.org/10.1016/S0020-7683(01)00103-2)
- [6] Li, S. G. & Kardomateas, G. A. (2008). Nonlinear response of a shallow: sandwich shell with compressible core to blast loading. *Journal of Applied Mechanics*, 75, 610-23. <https://doi.org/10.1115/1.2937154>
- [7] Ferri, E. A. & Deshpande, V. S. (2010). The dynamic strength of a representative double layer prismatic core: a combined experimental, numerical, and analytical assessment. *Journal of Applied Mechanics*, 77(1), 610-11. <https://doi.org/10.1115/1.4000905>
- [8] Belingardi, D. R. & Cavatorta, M. P. (2003). Material characterization of a composite-foam sandwich for the front



- structure of a high speed train. *Composite Structures*, 61(1), 13-25. [https://doi.org/10.1016/S0263-8223\(03\)00028-X](https://doi.org/10.1016/S0263-8223(03)00028-X)
- [9] Kazemi, M., Ghahri Saremi, T., & Ghahri Saremi, T. (2023). Resistance of Cylindrical Sandwich Panels with Aluminum Foam under Blast Loading. *Tehnički vjesnik*, 30(3), 765-770.
- [10] Kazemi, M. (2021). Experimental analysis of sandwich composite beams under three-point bending with an emphasis on the layering effects of foam core. *International Journal of Structures*, 29, 383-391. <https://doi.org/10.1016/j.istruc.2020.11.048>
- [11] Murrach, J. D. (2006). A qualitative assessment of blast damage and collapse patterns. *Journal of Performance of Constructed*, 20(1), 330-335. [https://doi.org/10.1061/\(ASCE\)0887-3828\(2006\)20:4\(330\)](https://doi.org/10.1061/(ASCE)0887-3828(2006)20:4(330))
- [12] Wadley, H. (2006). Multifunctional periodic cellular metals. *Mathematical, Physical and Engineering Sciences*, 364(1), 31-68. <https://doi.org/10.1098/rsta.2005.1697>
- [13] Hanssen, L. M. & Enstock, L. (2002). Close-range blast loading of aluminium foam panels. *International Journal of Impact Engineering*, 27(1), 593-618. [https://doi.org/10.1016/S0734-743X\(01\)00155-5](https://doi.org/10.1016/S0734-743X(01)00155-5)
- [14] Amini, N. S. & Isaacs, J. B. (2006). Effect of polyurea on the dynamic response of steel plates. *Conference Proceedings of the Society for Experimental Mechanics Series, USA*.
- [15] Dharmasena, H. J., Wadley, H. N., & Xue, G. Z. (2008). Mechanical response of metallic honeycomb sandwich panel structures to high-intensity dynamic loading. *International Journal of Impact Engineering*, 35(1), 1063-74. <https://doi.org/10.1016/j.ijimpeng.2007.06.008>
- [16] Wei, E. A. & Zok, F. W. (2006). Design of sandwich panels with prismatic cores. *Journal of Engineering Materials and Technology*, 128(1), 186-92. <https://doi.org/10.1115/1.2172279>
- [17] Rathbun, E. A. & Zok, F. W. (2005). Strength optimization of metallic sandwich panels subject to bending. *International Journal of Solids and Structures*, 42(1), 6643-61. <https://doi.org/10.1016/j.ijsolstr.2005.06.044>
- [18] Xue, H. J. (2003). Preliminary assessment of sandwich plates subject to blast loads. *International Journal of Mechanical Sciences*, 45(1), 687-705. [https://doi.org/10.1016/S0020-7403\(03\)00108-5](https://doi.org/10.1016/S0020-7403(03)00108-5)
- [19] Fleck, D. V. (2004) The resistance of clamped sandwich beams to shock loading. *Journal of Applied Mechanics*, 71(1), 386-401. <https://doi.org/10.1115/1.1629109>
- [20] Tilbrook, F. N. & Deshpande, F. N. (2006). The impulsive response of sandwich beams: analytical and numerical investigation of regimes of behavior. *Journal of the Mechanics and Physics of Solids*, 54(1), 2242-80. <https://doi.org/10.1016/j.jmps.2006.07.001>
- [21] Liang, M., Spuskanyuk, A. V., Flores, S. E., Hayhurst, D. R., & Hutchinson, J. W. (2007). The response of metallic sandwich panels to water blast. *Journal of Applied Mechanics*, 74(1), 81-99.
- [22] Evans, A. G. & Hutchinson, J. W. (2001). The topological Design of Multifunctional Cellular. *Progress in Materials Science*, 46(1), 309-327. [https://doi.org/10.1016/S0079-6425\(00\)00016-5](https://doi.org/10.1016/S0079-6425(00)00016-5)
- [23] Taheri-Behrooz, F. & Mansourinik, M. (2017). Experimental and numerical analysis of sandwich composite beam under four-point bending. *Modares Mechanical Engineering*, 17(1), 241-252.
- [24] Zarei Mahmoudabadi, M. & Sadighi, M. (2011). A study on the static and dynamic loading of the foam filled metal hexagonal honeycomb - Theoretical and experimental. *Materials Science and Engineering A*, 530(1), 333-343. <https://doi.org/10.1016/j.msea.2011.09.093>
- [25] Xiong, J., Vaziri, A., Ma, L., Papadopoulos, J., & Wu, L. (2012). Compression and impact testing of two-layer composite pyramidal-core sandwich panels. *Composite Structures*, 94(2), 793-801. <https://doi.org/10.1016/j.compstruct.2011.09.018>
- [26] Zhang, L., Hebert, R., Wright, J. T., Shukla, A., & Kim, J. H. (2014). Dynamic response of corrugated sandwich steel plates with graded cores. *International Journal of Impact Engineering*, 65(1), 185-194. <https://doi.org/10.1016/j.ijimpeng.2013.11.011>
- [27] Yan, L. L., Han, B., Yu, B., Chen, C. Q., Zhang, Q. C., & Lu, T. J. (2014). Three-point bending of sandwich beams with aluminum foam-filled corrugated cores. *Materials and Design*, 60(1), 510-519. <https://doi.org/10.1016/j.matdes.2014.04.014>

**Contact information:**

**Mahdi KAZEMI**, Professor (Assistant)  
(Corresponding author)  
Malayer University,  
65719-95863  
E-mail: kazemi@malayeru.ac.ir

**Alireza MIRZABIGI**, BSc Student  
Malayer University,  
65719-95863  
E-mail: alireza.kessb@gmail.com